Chapter

Forecasting and Modelling of Solar Radiation for Photovoltaic (PV) Systems

Ines Sansa and Najiba Mrabet Bellaaj

Abstract

Solar radiation is characterized by its fluctuation because it depends to different factors such as the day hour, the speed wind, the cloud cover and some other weather conditions. Certainly, this fluctuation can affect the PV power production and then its integration on the electrical micro grid. An accurate forecasting of solar radiation is so important to avoid these problems. In this chapter, the solar radiation is treated as time series and it is predicted using the Auto Regressive and Moving Average (ARMA) model. Based on the solar radiation forecasting results, the photovoltaic (PV) power is then forecasted. The choice of ARMA model has been carried out in order to exploit its own strength. This model is characterized by its flexibility and its ability to extract the useful statistical properties, for time series predictions, it is among the most used models. In this work, ARMA model is used to forecast the solar radiation one year in advance considering the weekly radiation averages. Simulation results have proven the effectiveness of ARMA model to forecast the small solar radiation fluctuations.

Keywords: solar radiation, PV power, forecasting, ARMA, fluctuation

1. Introduction

Solar energy is a renewable energy source, clean and inexhaustible. It is based on the photovoltaic effect to convert solar energy into electricity through solar cells. PV panels was mainly installing in isolated areas to provide them the electricity but in the last few years a considerable amount of electricity has been generated from solar energy in different countries in the world. In 2019, the global installed solar energy capacity has reached 586.42 GW [1]. This significant growth will may be continuing in the future due to its several technological, environmental and economic benefits.

Like some other renewable energies, solar energy is intermittent. Its production is so related to the solar radiation received on the earth. Therefore, it is possible to forecast solar energy from a relevant forecasting of solar radiation. Different techniques have been developed in the literature to forecast solar radiation. Most of them treat it as time series. These techniques are based on the historical solar radiation data, they treated and followed the solar radiation evolution on the past. Based on the historical data, a model is created to characterize the solar radiation behavior in the past. Therefore, the forecasting of solar radiation on a given time interval is based on this created model. The aim of this chapter is the forecasting of solar radiation using ARMA model. Based on these results and taking into account some other parameters, the PV power is then modeled. A general overview of solar radiation and its different propagation forms is presented in the first part of this chapter. Then, a brief literature review on solar radiation forecasting techniques will be the subject of the next part. After that, the ARMA model will be used to forecast the annual solar radiation corresponds to an industrial company by considering the weekly radiation averages. PV power is modeled in the following section and based on the forecasting solar radiation results, it is presented for different PV panels number. The end section concludes and summarizes this chapter.

2. General presentation of solar radiation

The sun is a vital element, necessary for photosynthesis, important for plants and fundamental for the thermal balance of different component of the crop. 75% of its composition is Hydrogen and the rest is Helium [2]. The sun is the primary source of electromagnetic radiation in Earth. It emits energy in the form of electromagnetic waves called solar radiation which mainly composed of visible light, ultra violet and infrared radiation. Visible light is the part of electromagnetic spectrum visible with the naked eye, its wavelength is depended to the individual. The ultra violet radiation is characterized by a wavelength greater than 800 nm, it is also called black light. This type of radiation is not visible with the naked eye. The infrared is a radiation with a wavelength less than 400 nm. It is greater than that of visible light but shorter than that of micro wave. When the solar radiation passes through the atmosphere, it is reduced due to its molecular scattering and its absorption by gas molecules. Ultra violet and infrared radiations are the two most absorbed. The amount of energy received on earth is depended to the atmosphere thickness and to some other factors such as the seasonal and cloud variations.

2.1 Propagation of solar radiation in the atmosphere

By propagating in the atmosphere, solar radiation can be diffused, absorbed or reflected,

- Reflected radiation: the radiation is reflected by the earth's surface and the soil reflects the radiation in a diffuse and anisotropic manner.

- Diffused radiation: the radiation is diffused in all direction, this phenomenon is occurred in a medium containing fine molecules and it strongly depends to these molecules size.

- Absorbed radiation: the radiation is absorbed by gas molecules that it encounters in atmosphere, this absorption is mainly due to water vapor, carbon dioxide and ozone.

These different interaction of solar radiation with atmosphere are recapitulated in the **Figure 1** [3].

2.2 Modeling of solar radiation

Several theories are developed in the literature to model solar radiation [4–6]. Therefore, at a specific moment and in a given location, the solar radiation cannot be modeled without requiring some factors such as the sky nature and the sun

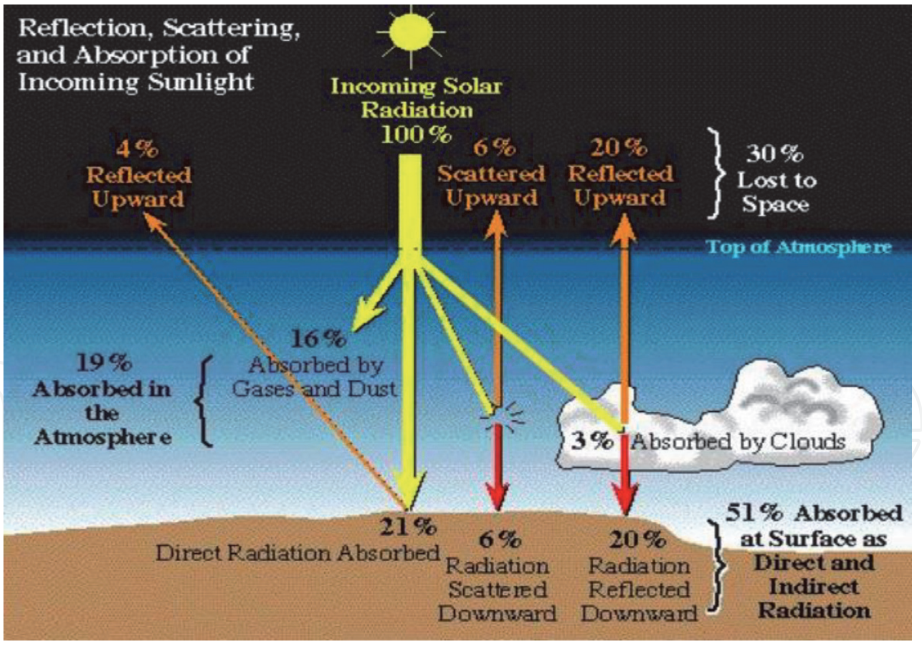

Figure 1.
Interaction between solar radiation and the atmosphere [3].

position. As mentioned previously, solar radiation has three different components, reflected, diffused and absorbed. All these components are modeled by the global or total solar radiation as presented in the Eq. (1).

$$R_{tot} = R_{dir} + R_{dif} + R_{ref} \tag{1}$$

With R_{tot} represents the total solar radiation, R_{dir}, R_{dif} and R_{ref} are respectively the directed, diffused and reflected solar radiation. Each of these radiations is sensitive to certain parameters and are calculated as presented in the following equations,

$$R_{dir} = Sh.Rout.\tau^{M}.\cos(i) \tag{2}$$

$$R_{diff} = Rout.\left(0.271 - 0.294.\tau^{M}\right).\sin(\alpha) \tag{3}$$

$$R_{ref} = r.Sc.\left(0.271 + 0.706.\tau^{M}\right).\sin(\alpha).\sin^{2}\left(\frac{x}{2}\right) \tag{4}$$

With Sh is a binary umbrage value, it is computed for each hour in day. Sh is assigned to 0 when the solar radiation is projected to the neighboring mountain umbrage, else it is assigned to 1. r represents the soil reflectance; it is also called the reflection factor. Sc is the constant solar equal to 1367 W/m^2. To define the other parameters, a recourse to the geometry between sun and earth as well as to the characteristics of the solar flux are needed. Indeed, the position of the sun in the sky depends to the time and latitude. It is defined by two angles which characterized the altitude and the solar azimuth. The altitude angle α is defined as presented in the below Eq. [7].

$$\sin\alpha = \sin\varphi.\sin(\delta) + \cos(\varphi).\cos(\eta) \tag{5}$$

With φ and η are respectively the latitude for each cell and the solar time. δ represents the solar declinaition, this parameter depends to the year day j and expressed as written in Eq. (6),

$$\delta = 23.45.\sin\left(360.\frac{284 + j}{365}\right) \tag{6}$$

The azimuth angle β is defined as presented in the Eq. (7)

$$\cos\beta = (\sin\delta.\cos\varphi - \cos\delta.\sin\varphi.\cos\eta)/\cos\alpha \tag{7}$$

Rout represents the solar flux, it depends to the solar constant Sc and the year day j, it is written as indicated in the Eq. (8),

$$\text{Rout} = \text{Sc.}\left(1 + 0.034.\cos\left(\frac{360j}{365}\right)\right) \tag{8}$$

τ^M represents the transmissivity coefficient, it is defined as the fraction of the solar radiation incident on the atmosphere surface that reaches the soil along a vertical trajectory. In the mountain area, a correlation factor linked to the atmospheric pressure p/p0 must be used. The path length is presented by the lettre M and written as shown in the Eq. (9),

$$M = M_0.\frac{P}{P_0} \tag{9}$$

M_0 is calculated following the Eq. (10) and the p/p0 represents the correlation factor of atmospheric pressure, it is calculated as defined in the Eq. (11).

$$M_0 = \sqrt{1229 + (614.\sin\alpha)^2} - (614.\sin\alpha) \tag{10}$$

$$\frac{P}{P_0} = \left(\frac{288 - 0.0065.h}{288}\right)^{5.256} \tag{11}$$

An incidence angle i between the sun ray and the soil surface must be taken into account when the solar radiation is converged to sloping areas. This angle is depended to the sun position and to the topography and it is written as described the below equation,

$$\cos i = \cos\alpha.\sin x.\cos(\beta - \beta_s) + \sin\alpha.\cos x \tag{12}$$

With x and β_s represent respectively the slope and the exposure, they are taken in degrees. It should be noted that the Eq. (1) describes the solar radiation without taking into account the clouds effects. To take them into account, a coefficient Kc must be added. So the expression of solar radiation in the presence of clouds R_{totc} will be written as presented in the Eq. (13).

$$R_{totc} = K_c.R_{tot} \tag{13}$$

The K_c coefficient is depended to the cloudiness N and calculated as described in the Eq. (14).

$$K_c = \left(1 - 0.75.\left(\frac{N}{8}\right)^{3.4}\right) \tag{14}$$

3. Forecasting of solar radiation

3.1 Forecast horizon

Before forecasting, it must specify firstly the horizon forecasting. The choice of this horizon is relative to the problem to be treated. They are four forecasting horizon categories which are the very short term, the short term, the medium term and the long term. Each of these horizons is characterized by a time interval as described in the following paragraph,

- Very short term: the time horizon of this forecasting category does not exceed a few hours, usually it is used for the intra-day market.
- Short term: the time horizon of this category is between 48 hours and 72 hours. This type of forecasting horizon is useful for the daily dispatching electrical power.
- Medium term: the time horizon of this forecasting term is done for more than one week to one month. It intervenes in the planning of the power system. It is also used for the dispatching of the conventional power plants.
- Long term: the time horizon of this type is done from one month to one year. It is useful for long term planning operations such as expansion projects for power generation units.

3.2 Solar radiation forecasting techniques

In the literature, different techniques are proposed to the forecasting of solar radiation [7]. It is possible to classify them into four groups, the naïve models, the conditional probability models, the reference models and the connectionist models. A description of each of these techniques is described in the following sub sections.

3.2.1 Naïve model

They are the smallest techniques for time series forecasting. For a given horizon, the forecasting is based on the last observed variable [8]. The mean, the persistence and the k nearest neighbors are registered under these models.

3.2.1.1 Mean forecasting method

The mean forecasting method consists to substitute the variable to be forecasted by the mean available data assigned to this variable. It is a simple technique to apply but it is so expensive in terms of history [7]. If N corresponds to the number of historical data, the forecasting of a variable x at a given horizon h is described as presented in the Eq. (15).

$$\hat{x}_{t+h} = \frac{1}{N}\sum_{i=1}^{N} x_i \tag{15}$$

3.2.1.2 The persistence

This technique is based on the repetition of a measurement from time t to time t+h [7]. If the considered horizon h is 1, the forecasting of a variable data at time time t+1 is defined as written in the Eq. (16).

$$\hat{x}(t+1) = x(t) \tag{16}$$

This predictor type is often used in time series forecasting because it is so easy to implement and it does not require a large historical data base. On the other hand, it is imprecise and it does not lead to an improvement in time series.

3.2.1.3 The k nearest neighbors

This technique is derived from the artificial intelligence, it consists to find in time series, a set of k data similar to those that to be predicted [9]. The determination of k is done by different algorithm [7]. This technique is, in general, efficient in the time series forecasting, however, it is sensitive to the dimensionality and to the irrelevant variables.

3.2.2 Conditional probability models

We cite as an example for these types of models those of Marcov chains and Bayesian inferences.

3.2.2.1 Marcov chain

This technique is rarely used for the forecasting of solar radiation [10]. It is a stochastic process that has the Markovian property [11]. A future state is modeled by a probabilistic process which depends only to the present states. Following Markov chain, the forecasting of a variable at a given horizon h is defined as presented in the Eq. (17).

$$X_{t+h} = X_t . R_M^h \tag{17}$$

With R_M represents the transition matrix of Markov chain, its dimension depends to several factors such as the number of available data and the precision nature [12].

3.2.2.2 Bayesian inferences

This method is mainly based on the conditional probability; it is rarely used for the forecasting of solar radiation. This method is very difficult to handle and it requires several parameters. The estimation of the probability of a series at a given horizon can be done by Bayes theorem as described in the Eq. (18).

$$p\left({}^{A}\!/\!{}_{B}\right) = \frac{p\left({}^{B}\!/\!{}_{A}\right).p(A)}{p(B)} \tag{18}$$

3.2.3 Connectionist models

The first artificial neuron was created by Warren McCulloch and Walter Pitts in 1943 [13]. The structure of this neuron is imitated from the biological neuron as presented in the **Figure 2** [14]. An artificial neural network (ANN), is an assembly strongly connected of formal neurons. It is characterized by an excellent capacity of learning and generalization as well as a speed of processing. Its ability to learn and generalize makes it a very powerful tools. It has proven, in recent years, its effectiveness in various research fields. ANNs are subdivided into two large families, static and dynamic neural network. The choice of the one or the other of these two networks depends to the application to be processed, the available information and the complexity model [15].

3.2.4 Conditional probability models

These are models from the large family of Auto Regressive and Moving Average (ARMA). ARMA is the combination of two models, the Auto Regressive (AR) and Moving Average (MA). It is characterized by its ability to extract useful statistical properties. Thus, it is among the most widely used models for time series forecasting. Its effectiveness to forecast solar radiation is well proven in certain research work [16]. AR model assumes that each point can be forecasted by the sum of p previous points plus a random error term. The expression of AR model with an order p (AR (p)) is written as presented in the Eq. (19),

$$x(t) = \alpha_1.x(t-1) + \alpha_2.x(t-2) + \ldots \alpha_p.x(t-p) + \varepsilon_t \tag{19}$$

with α_i represent the AR coefficients and ε_t is a white noise.

The moving average process assumes that each point is the sum of q previous errors plus its own error. The expression of MA model with an order q (MA(q)) is written as presented in the Eq. (20).

$$x(t) = \beta_1.e(t-1) + \beta_2.e(t-2) + \ldots \beta_q.e(t-q) \tag{20}$$

With β_i are the MA coefficients. A combination of these two models forms the ARMA model with order p and q, its expression is described in the Eq. (21).

$$\begin{aligned} x(t) = {} & \alpha_1.x(t-1) + \alpha_2.x(t-2) + \ldots \alpha_p.x(t-p) + \beta_1.e(t-1) \\ & + \beta_2.e(t-2) \ldots \beta_q.e(t-q) + \varepsilon_t \end{aligned} \tag{21}$$

The major requirement of ARMA model is that the time series studied must be stationary. A series is considered stationary when its statistical properties such the mean and the variance are constant over time [17]. The distribution of a stationary series at time t is identical to that at time t-1. The unit root is among the stationarity tests. Autos-correlations and partial autos-correlations diagrams can be used also to prove the stationarity of time series.

If the time series is proved stationary, an approach must be followed to define the p and q orders. Box and Jenkins methodology is used to determine them, it contains four steps, identification of the model, estimation of the parameters, the validation of the selected model and finally the use of this model for forecasting.

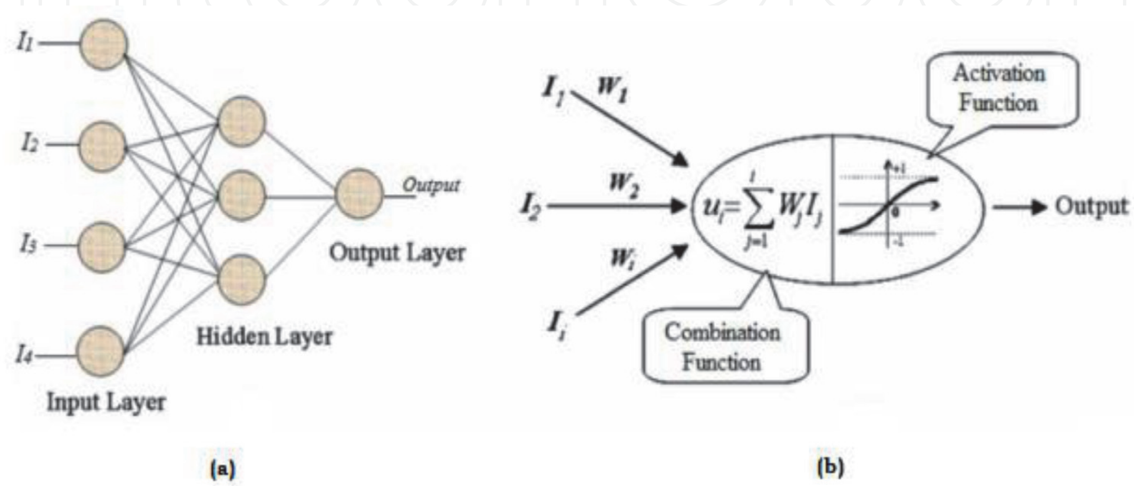

Figure 2.
Schematic diagram of an ANN structure neuron model [14].

- Identification: this is the most important step, it aims to identify the p and q orders. This is done by examining the auto correlation and the partial auto correlation diagrams of the time series.

- Estimation of parameters: the determination of p and q orders does not reflect the validation of this model. It is necessary to estimate the ARMA(p,q) selected. This estimation can be made by the student test.

- Validation model: this validation is carried out by applying two tests on the residues, the Ljung-Box test and homoscedasticity test to ensure that the residuals are white noises.

- The use of model: the selected ARMA model can be used in forecasting. However, in order to ensure the validity of this model, it must be tested on a data base already known. It should find good forecasting performances by comparing the data forecasted by this model and those already known.

3.3 Solar radiation forecasting using ARMA model

The objective of this section is to forecast the solar radiation using ARMA model. The data base solar radiation considered for the forecasting is the set of solar radiation measurements corresponds to an industrial company located in Barcelona north [18]. The time interval of these measurements is five minutes, they are taken every day for a whole year as presented in the **Figure 3**.

To refine the representative curve, just the weekly solar radiation averages are taken into account as presented in the **Figure 4**.

To apply ARMA model, it must study the stationarity of this series. Correlograms corresponding to the auto-correlations and to the partial auto-correlation to this series are presented in the **Figure 5**.

The auto-correlation coefficient of order 1 is close to 1 and the correlogram shows a slow regression which is typical of non-stationary series. Dickey Fuller test is thus applied using EViews software; it proves the weak stationary of this series as shows in the **Figure 6**.

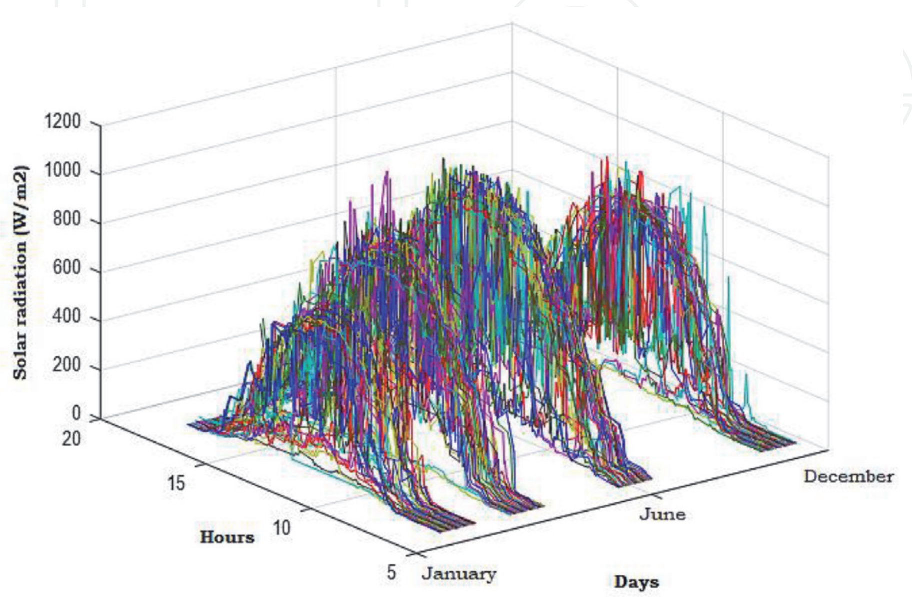

Figure 3.
Annual solar radiation evolution.

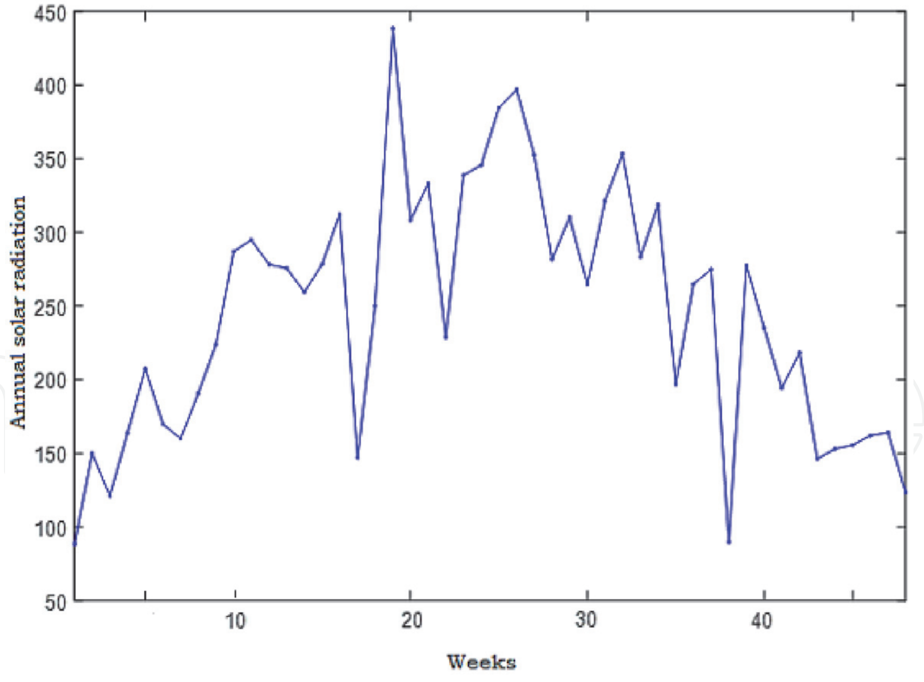

Figure 4.
Weekly solar radiation averages.

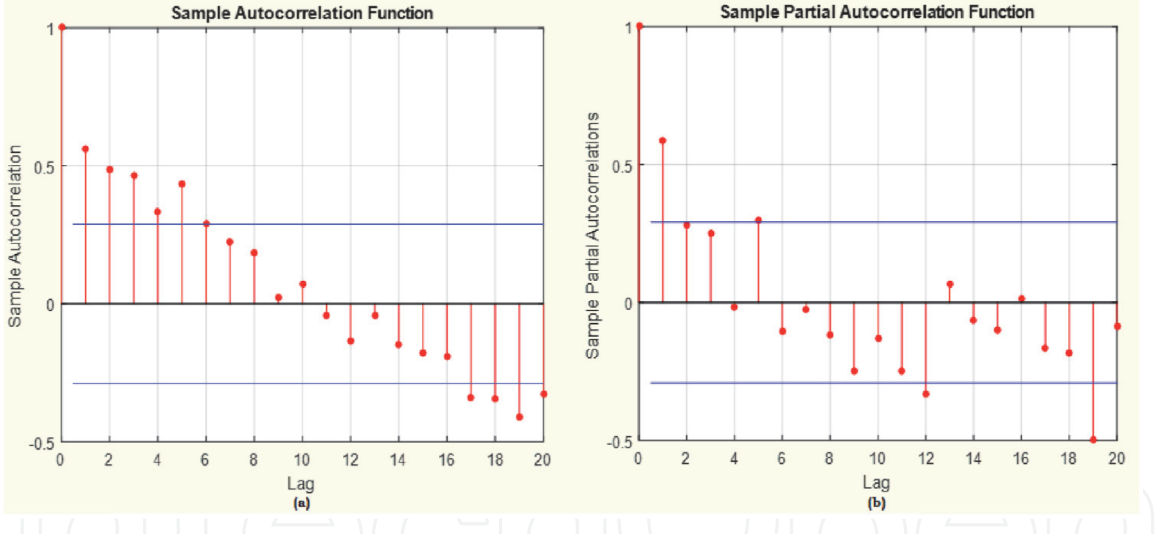

Figure 5.
(a) Auto-correlation and partial auto-correlation (b) correlograms of annual solar radiation.

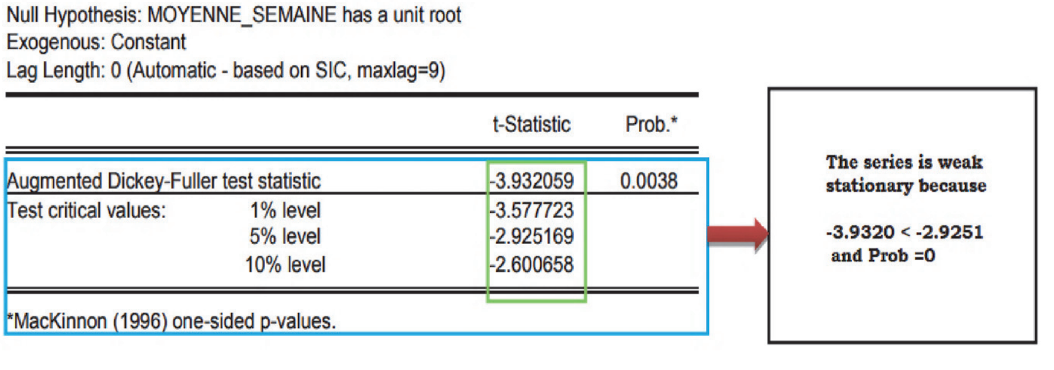

Null Hypothesis: MOYENNE_SEMAINE has a unit root
Exogenous: Constant
Lag Length: 0 (Automatic - based on SIC, maxlag=9)

		t-Statistic	Prob.*
Augmented Dickey-Fuller test statistic		-3.932059	0.0038
Test critical values:	1% level	-3.577723	
	5% level	-2.925169	
	10% level	-2.600658	

*MacKinnon (1996) one-sided p-values.

Figure 6.
Dickey fuller test results for weekly solar radiation series.

The differentiation of this series is necessary in order to make it stationary. The following **Figure 7** shows the evolution of the differentiated weekly solar radiation.

The Dickey Fuller is thus applied and it proves the stationary of this series as shown in the **Figure 8**. Thereafter, the different Box and Jenkins methodology steps are followed to obtain finally the optimal ARMA model that reproduces the best the behavior of this series. Orders p and q, coefficients α_1, α_2 and β_1 of the ARMA model are recapitulated in the **Table 1**.

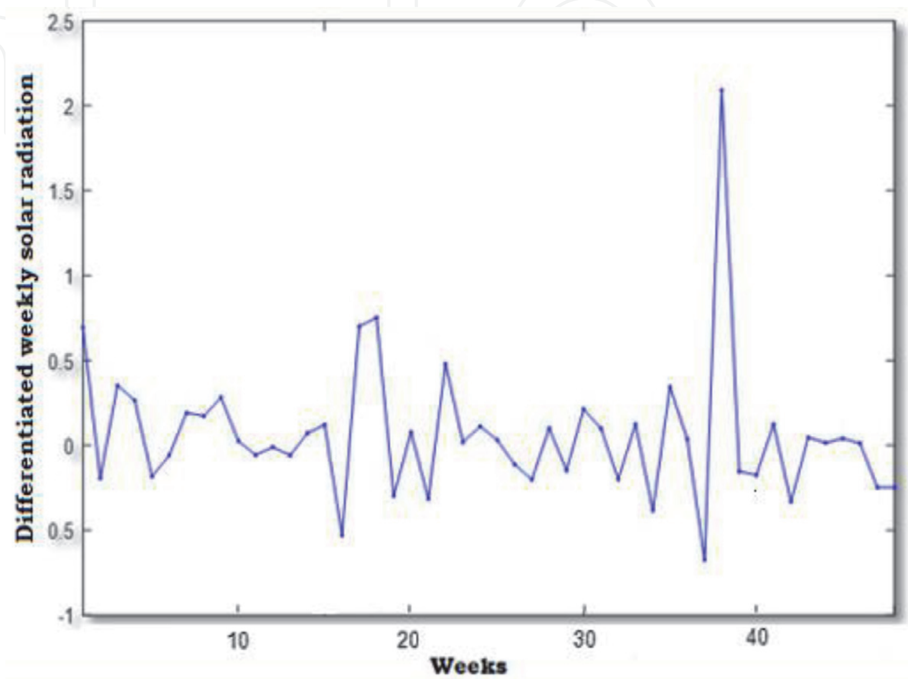

Figure 7.
Differentiated weekly solar radiation evolution.

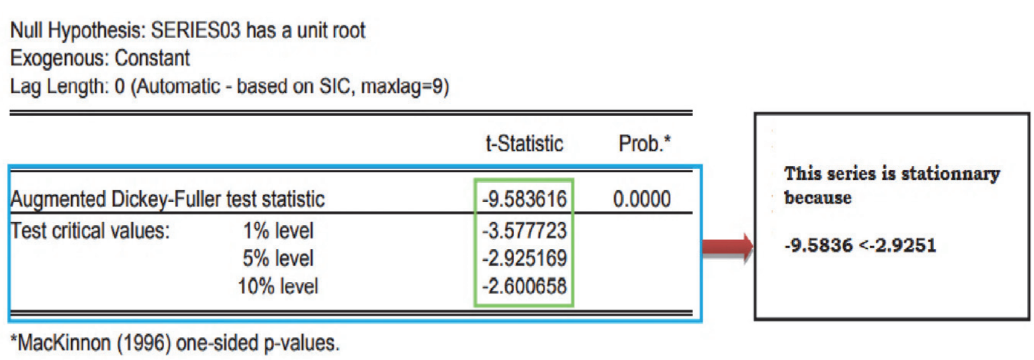

Null Hypothesis: SERIES03 has a unit root
Exogenous: Constant
Lag Length: 0 (Automatic - based on SIC, maxlag=9)

		t-Statistic	Prob.*
Augmented Dickey-Fuller test statistic		-9.583616	0.0000
Test critical values:	1% level	-3.577723	
	5% level	-2.925169	
	10% level	-2.600658	

*MacKinnon (1996) one-sided p-values.

This series is stationnary because

-9.5836 <-2.9251

Figure 8.
Dickey fuller test results for the differentiated weekly solar radiation series.

ARMA (p,q)	
Order	**Coefficients**
p = 2	$\alpha_1 = -1.0342$; $\alpha_2 = -0.4023$
q = 1	$\beta 1 = 0.7483$

Table 1.
Orders and coefficients of ARMA (2,1).

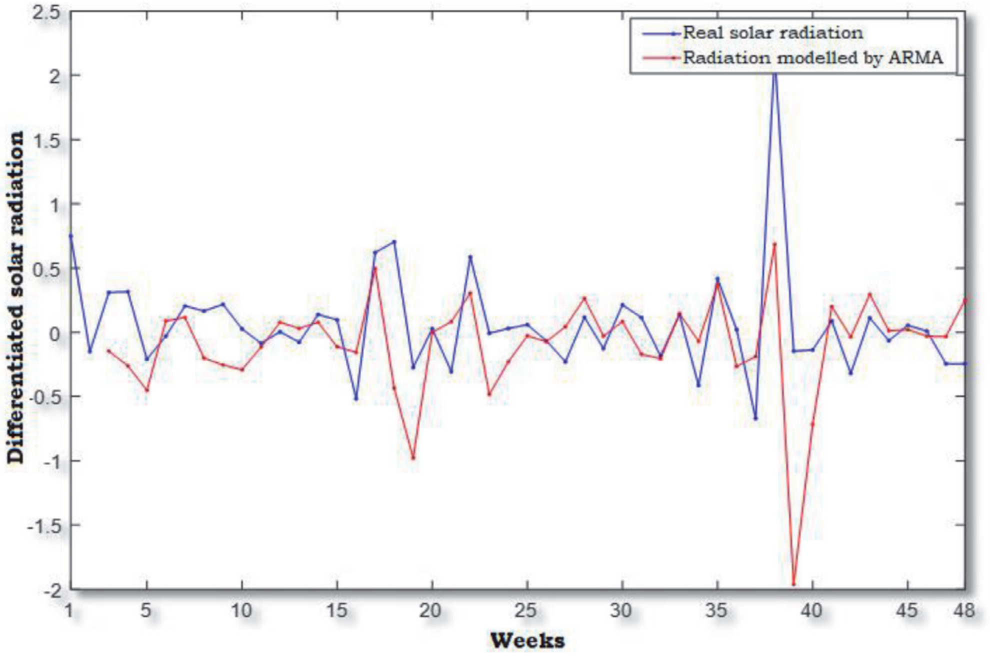

Figure 9.
Solar radiation modeled by ARMA (2,1).

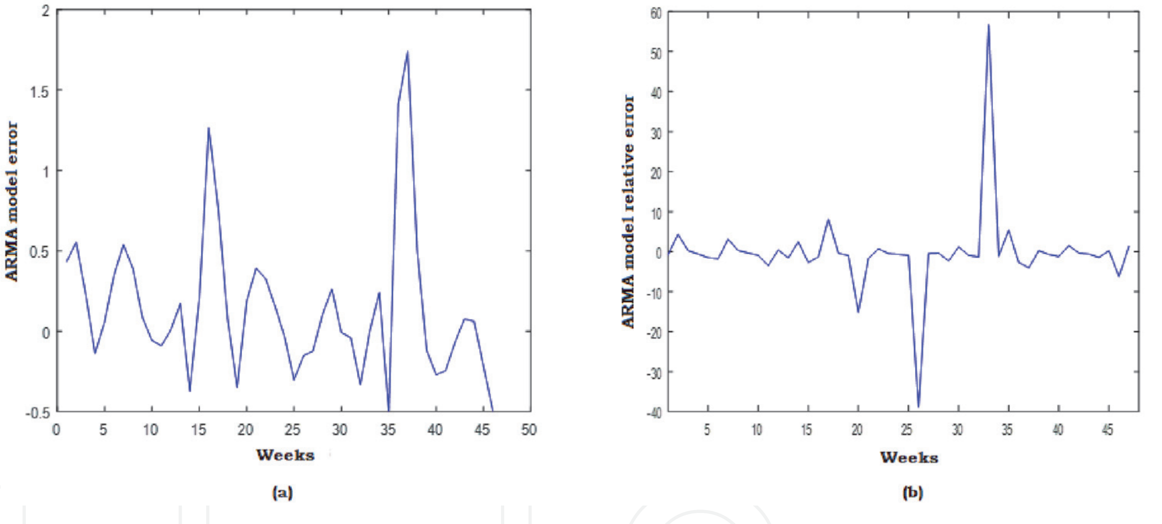

Figure 10.
Error (a) and relative error (b) of solar radiation modeled by ARMA (2,1).

In this paragraph, ARMA (2,1) model is used to forecast the differentiated weekly solar radiation averages. The real solar radiation curve and the forecasted one are presented in the **Figure 9**. It is clear that an approximation is observed between the two curves for certain time intervals, especially when the solar radiation does not present large fluctuations. For other moments time, the forecasted solar radiation curve diverges from the real one. This is particularly observed when the solar radiation presents large fluctuations. To confirm these results, the ARMA model errors are presented in **Figure 10**.

Following the **Figure 10b**, it is clear that the relative error is small, it does not exceed 15%. It is thus observed two peaks, the first one corresponds to the 16th week of the year and the second is in the 36th week. Therefore, when we refer to the real annual solar radiation curve, we observe a sudden fluctuation during these two weeks. Indeed, 16th and 17th weeks correspond respectively to the last week of April month and the first week of May. A considerable decrease of temperature is

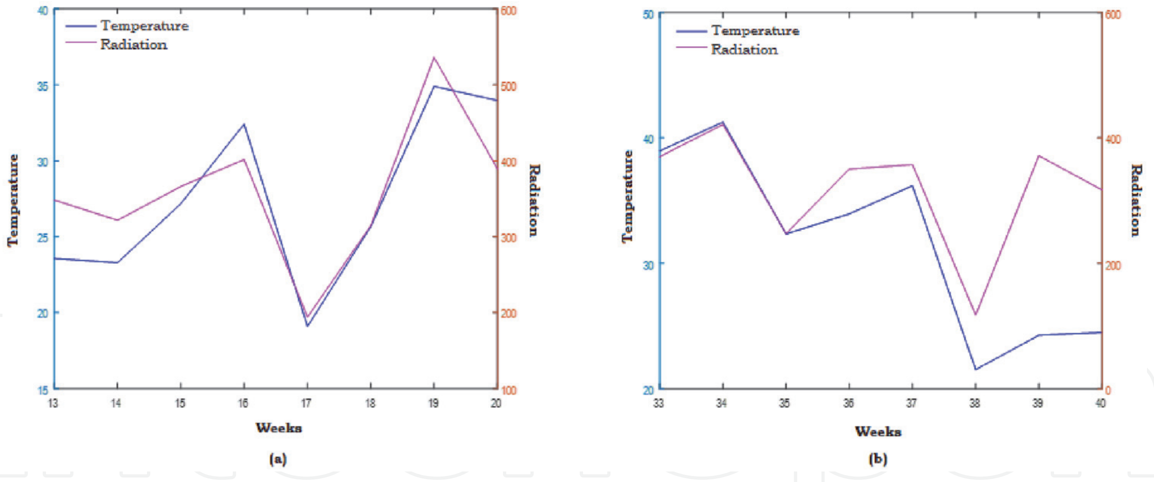

Figure 11.
Influence of temperature on solar radiation (a) April and may weeks (b) September and October weeks.

Errors	Performances
MSE	0.2182
MAE	0.2999
RMSE	0.4671

Table 2.
Errors of solar radiation forecasting using ARMA (2,1).

observed during this period; this is may be the main reason to the sudden decrease of radiation. On the other hand, 37th and 38th weeks correspond to the two first weeks of September month. At the end of this period, it is observed also a sudden decrease of the temperature which affects considerably the solar radiation. Furthermore, as the weekly solar radiation averages are considered for the forecasting, it is obvious to have these large solar radiation variations especially in the switching periods from one season to another one. The influence of temperature on solar radiation evolution for April, May, September and October months are presented in the **Figure 11**.

After forecasting solar radiation or any other parameters, a forecasting error should always be calculated. An error in the forecasting context does not indicate a fault or an anomaly as it is known in several other fields but rather a criterion to evaluate the forecasting performances. In this study, Mean Square Error (MSE), Mean Absolute Error (MAE) and Root Mean Square Error (RMSE) are calculated as written in the Eqs. (22)–(24) [19]. $e_{i\ (i=1\ldots n)}$ represents the error measured between the actual value and the forecasted one for sample i and n is the total number of samples. Results are recapitulated in the **Table 2**, the MSE presents the lowest one (0.2182), it is a small value which reflects the performances of ARMA (2,1) model to forecast the solar radiation.

$$\mathrm{MSE} = \frac{1}{n}\sum_{i=1}^{n} e_i^2 \tag{22}$$

$$\mathrm{RMSE} = \sqrt{\frac{1}{n}\sum\nolimits_{i=1}^{n} e_i^2} \tag{23}$$

$$\mathrm{MAE} = \frac{1}{n}\sum\nolimits_{i=1}^{n} |e_i| \tag{24}$$

4. Modeling and forecasting of PV power

The forecasting of PV power has a great importance to the best management of grid connected PV systems as well as to the isolated micro grid which include PV system as renewable energy source. Based on the literature, it is possible to forecast the PV power by direct or indirect methods [20]. Direct methods consist to describe models to directly forecast the amount of PV power or forecast the PV power without using other metrological data. In this context, different approaches are suggested which mainly the ANN and the machine learning techniques [20–22]. On the other hand, the indirect methods consist to forecast the PV power based on the forecasting of another meteorological data such as the solar radiation or the temperature [20, 23]. Different physical and statistical approaches are proposed in this field. The choice for the one or the other method is depended to the available data and the forecast horizon term. In physical approaches, the PV power forecasting is based on weather variables predicted by numerical weather prediction (NWP) models and they are more suitable for the long term horizon. The statistical approaches are based on past measured time data series and generally they are appropriate for short term horizon. Moreover, the statistical approaches are simpler than the physical approaches since they require less input data and lower computation [24].

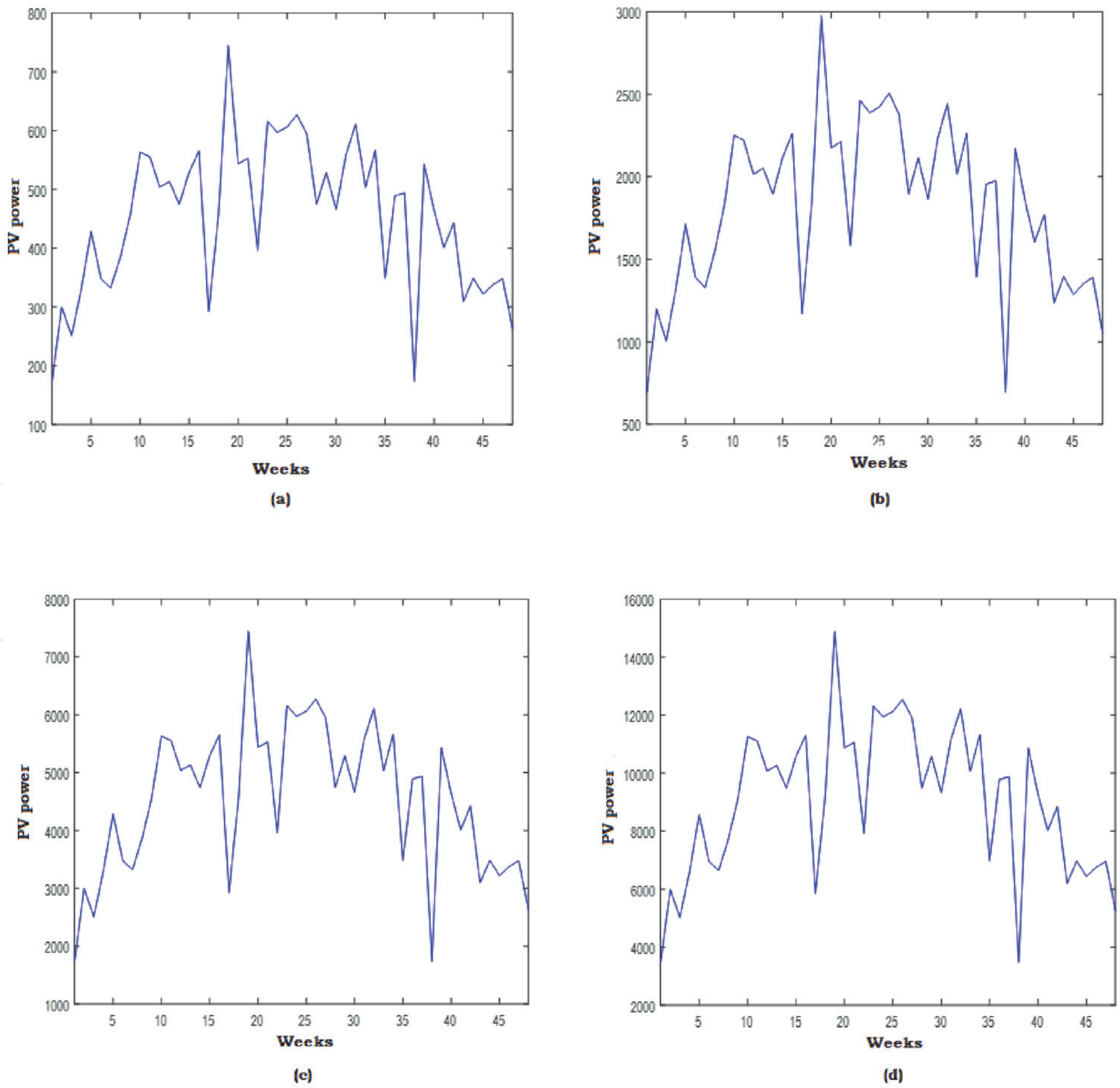

Figure 12.
PV power forecasting for different PV panels number (a) N=5 (b) N=20 (c) N=50 (d) N=100.

In the following section, the PV power will be modeled and forecasted based on the results of solar radiation forecasting, presented in the precedent section. Indeed, the PV power generators are very often operating with a maximum power called Maximum Power Point Tracker (MPPT) [25]. The maximum power P_{PV} delivered by a PV generator composed of N PV panels can be expressed as indicated in the Eq. (25) [26].

$$P_{PV} = \eta_g.N.A.G \tag{25}$$

With A represents the area of a single PV panel, it is expressed in m^2. G is the solar radiation measured in w/m^2. η_g is the PV generator efficiency and it is described as written in the Eq. (26) [27].

$$\eta_g = \eta_r.\eta_{pt}.[1 - \beta_t.(T_c - T_r)] \tag{26}$$

η_r represents the reference efficiency of PV generator, it depends to the PV cells materials. η_{pt} is the efficiency of power tracking equipment, it is equal to 1 if the MPPT is perfectly used, β_t is the temperature coefficient, it is expressed in °C. The typical value of this coefficient varies between 0.004 and 0.006, usually, it is taken in the range of 0.005°C [26]. T_c and T_r represent respectively the tcemperature measured in the PV cells and the reference temperature. T_c depends to the ambient temperature T_a and the radiation G as presented in the Eq. (27) [26].

$$T_c = T_a + G.\frac{\mathbf{NOCT} - 20}{800} \tag{27}$$

The typical NOCT value for polycrystalline cells is around 45°C. Taking into account Eq. (26) and Eq. (27), the PV power is described as presented in the Eq. (28).

$$P_{PV} = \eta_r.\eta_{pt}.\left[1 - \beta_t.\left(T_a + G.\frac{\mathbf{NOCT} - 20}{800} - T_r\right)\right].N.A.G \tag{28}$$

As shown in the Eq. (28), the evolution of PV power depends to several parameters such as the temperature, the solar radiation and the PV panels number. Therefore, it is possible to forecast the PV power from the solar radiation forecasting. So, if the PV cells used is the pollicrystalline and the area of a single PV panel is $2.25m^2$, the evolution of PV power for different PV panels number and based on the solar radiation forecasting results is described as presented in the **Figure 12**.

5. Conclusion

This chapter focuses to model and to forecast the PV power based on the solar radiation forecasting results. Some physical equations are presented firstly to define in general the three different forms of solar radiation. They are explained taking into account some topographical factors and geometric relations.

For solar radiation forecasting, a set of solar radiation measurements corresponds to an industrial company is considered as data base. ARMA model is used to forecast the weekly solar radiation averages. The simulation results obtained are proven the effectiveness of this model to forecast the small variation of solar radiation. On the other hand, it is observed the deterioration of ARMA model with the large solar radiation fluctuations. The forecasting of PV power is carried out based on the obtained solar radiation forecasting results and taking into account some other parameters such as the temperature, the PV cells materials and the PV panels number.

Acknowledgements

This work was supported by Tunisian Ministry of Higher Education and Scientific Research under Grant LSE-ENIT-LR 11ES15.

Author details

Ines Sansa[1]* and Najiba Mrabet Bellaaj[2]

1 Université de Tunis El Manar, Ecole Nationale d'Ingénieurs de Tunis, LR11ES15, Laboratoire des Systèmes Electriques, Tunis, Tunisie

2 Université de Tunis El Manar, Institut Supérieur d'Informatique, Ariana, Tunisie

*Address all correspondence to: sansa.ines@yahoo.com

References

[1] Statistical Review of World Energy, https://www.bp.com/en/global/corporate/energy-economics/statistical-review-of-world-energy.html

[2] RJ. Aguiar, M. Collares-Pereira, JP. Conde: Simple procedure for generating sequences of daily radiation values using a library of Markov transition matrices, Solar Energy n°40(3), pp 269-279, 1988.

[3] Sultana N. Nahar: Solar irradiation of the earth's atmosphere, Department of Astronomy, the Ohio State University, Columbus, Ohio, USA.

[4] K. Liou: An introduction to atmospheric radiation. Academic Press, 2nd Edition ELSEVIER STORE, http://store.elsevier.com/An-Introduction-to-Atmospheric Radiation/K_-N_-Liou/isbn-9780080491677/

[5] F. Kasten: The Linke Turbidity Factor Based on Improved Values of the Integral Rayleigh Optical Thickness, Solar Energy n°56(3), Pp 239–244, 1996.

[6] V. Badescu: Modeling Solar Radiation at the earth's Surface: Recent Advances, Springer, 2008.

[7] C. Voyant: Prédiction de séries temporelles de rayonnement solaire global et de production d'énergie photovoltaïque à partir de réseaux de neurones artificiels, Thèse de doctorat, Spécialité Energétique, Novembre 2011.

[8] L. Ferrara: Méthodes autoprojectives de prévision des séries chronologiques, Modélisation Appliquée Polycopié de Cours, Université Paris Ouest, Février 2011.

[9] M. Sharif, D.H. Burn: Simulating climate change scenarios using an improved k nearest neighbor model, Journal of hydrology, pp. 179-196, 2006.

[10] C. Paoli, C. Voyant, M. Muselli, M. L. Nivet: Multi-horizon irradiation forecasting for Mediterranean locations using time series models, ISES Solar World Congress, 2013

[11] M. Muselli, P. Poggi, G. Notton: A. Louche first order Markov chain model for generating synthetic "typical days" series of global irradiation in order to design PV stand alone systems, Energy conversion and management, Vol 42-6, pp. 675-687, 2001.

[12] C. Piedallu, J.C. Gégout: Multiscale computation of solar radiation for predictive vegetation modelling, Annals of Forest Science 64, pp. 899-909, 2007.

[13] N. Mrabet Bellaaj: Contribution à l'identification et à la commande numériques de la machine asynchrone Algorithmes Génétiques, Réseaux de Neurones et Logique Floue, Thése de doctorat de l'Ecole Nationale d'Ingénieurs de Tunis, 2001.

[14] Utpal Kumar. Dasa, Kok Soon. Teya, Mehdi. Seyedmahmoudiana, Saad. Mekhilefb, Moh Yamani. Idna Idrisc, Willem van. Deventerc, bend. Horanc, Alex. Stojcevski: Forecasting of photovoltaic power generation and model optimization: A review, Renewable and Sustainable Energy Reviews 81, pp. 912-928, 2018.

[15] G. Salah Eddine: Identification des Systèmes non Linéaires par réseaux de neurones, Mastère en Automatique, Université Mohamed Khider-Biskra, Faculté des Sciences et de la technologie, Département: Génie électrique

[16] J. Wu, C.K. Chan: Prediction of hourly solar radiation using a novel hybrid model of ARMA and TDNN, Solar Energy 85, pp. 808-817, 2011.

[17] K. Thibodeau: Application de la méthodologie Box-Jenkins aux séries du ministère de la santé, Maîtrise en Mathématiques et Informatique

Appliquées, Université du Québec, Avril 2011.

[18] Sant Joan les Fonts, Garrotxa, http://www.noel.es/

[19] Ines SANSA: Optimization d'un micro reseau electrique selon la charge d'un site isolé et prediction de la puissance PV, thèse de Doctorat de l'école nationale d'ingenieurs de Tunis.

[20] Abdelhakim. El hendouzi, Abdennaser. Bourouhou: Solar Photovoltaic Power Forecasting, Journal of Electrical and Computer Engineering, 2020.

[21] R. Ahmed, V. Sreeram, Y. Mishra, M. D. Arif: A review and evaluation of the state-of-the-art in PV solar power forecasting: Techniques and optimization, Renewable and Sustainable Energy Reviews, vol. 124, 2020.

[22] Mellit, A. Massi Pavan, E. Ogliari, S. Leva, V. Lughi: Advanced methods for photovoltaic output power forecasting: A review, Applied Sciences, vol. 10, no 2, pp. 487, 2020

[23] J. Antonanzas, N. Osorio, R. Escobar, R. Urraca, F. J. Martinez-de-Pison, F. Antonanzas-Torres: Review of photovoltaic power forecasting, Solar Energy, vol. 136, pp. 78–111, 2016.

[24] Maria. Grazia De Giorg, Paolo Maria. Congedo, Maria. Malvoni: Photovoltaic Power Forecasting Using Statistical Methods: Impact of weather data, IET Science Measurement and Technology, May 2014.

[25] T. Logenthiran, D. Srinivasan, A. M. Khambadkone, T. S.raj: Optimal sizing of an islanded microgrid using evolutionary strategy, IEEE International Conference on Congress on Evolutionary Computation (CEC) Probabilistic Methods Applied to Power Systems (PMAPS), 2010.

[26] S. Missaoui: Prédiction de la production de la puissance PV à l'aide des réseaux de neurones dynamiques. Mastère en Systèmes Electriques, ENIT, Juillet 2012.

[27] D. Abbes, A. Martinez, G. Champenois: Life cycle cost, embodied energy and loss of power supply probability for the optimal design of hybrid power systems, Mathematics and Computers in simulation, 2013.